Available online at www.sciencedirect.com
ScienceDirect
Journal of the European Ceramic Society 28 (2008) 199–204
www.elsevier.com/locate/jeurceramsoc

Tribological properties of pressureless sintered alumina matrix ceramic materials improved by diopside

Changxia Liu [a,b,1], Jianhua Zhang [a,*], Junlong Sun [b], Xihua Zhang [c]

[a] *Department of Mechanical Engineering, Shandong University, Jinan 250061, Shandong Province, PR China*
[b] *Communications Institute, Ludong University, Yantai 264025, Shandong Province, PR China*
[c] *Department of Materials Science and Engineering, Shandong University, Jinan 250061, Shandong Province, PR China*

Received 5 February 2007; received in revised form 5 May 2007; accepted 13 May 2007
Available online 27 August 2007

Abstract

In this paper, diopside was introduced into alumina as a sintering aid and fine structural alumina matrix ceramic materials were fabricated by the technology of pressureless sintering. The relative density, hardness and fracture toughness of the diopside-reinforced composites were investigated. Tribological tests were carried out at a rotation speed ranged from 40 to 160 rpm and in a normal load ranged from 50 to 200 N. SEM technique was employed to observe worn surfaces of the test specimens and wear mechanisms were simultaneously discussed. Analysis of the experimental data and observations on worn surfaces revealed that the improvement in wear resistance of composites may be attributed mainly to the stronger toughening effect due to addition of diopside in alumina matrix.

Keywords: Al_2O_3; Diopside; Pressureless sintering; Friction and wear

1. Introduction

Major challenges in advanced structural ceramics such as manufacture reproducible, long lifetime, self-lubricating are always proposed in mechanical systems that involve high loads, velocities and temperatures. Advanced structural ceramics are widely applied in the fields of fine measuring implement, fine sliding way, working platform and high-speed bearing, etc., where high precision durability and long working life are required. Among these advanced ceramics, fine alumina matrix ceramic materials are widely selected due to their virtues of high hardness, good chemical inertness, high wear resistance, low coefficient of thermal expansion and friction coefficient. However, processing and manufacturing of pure alumina products is an expensive and difficult task. In our recent studies, the introduction of diopside into alumina matrix can decrease the manufacturing costs, shorten production cycle and improve mechanical properties.[1] However, few articles reported the tribological properties of the diopside-reinforced fine alumina matrix ceramic composites.[2]

Wear generally increases with normal contact load, sliding distance and sliding velocities, and a wear rate of 10^{-15} $m^3/N\,m$ is usually set as limit above which a material is no longer considered wear-resistant.[3] Numerous investigations exploring the influences of test conditions contact geometry, additives and environment on the tribological behaviour of alumina matrix ceramics exist, due to their growing importance for high wear resistance application.[4–7] In this investigation, the influences of rotation speed and load values on the friction and wear behaviour of fine alumina matrix ceramic materials toughened by diopside are studied and explored.

2. Experimental procedure

2.1. Materials and specimens

High purity of 99.99% α-Al_2O_3 with grain size of 0.5–1 μm and diopside ($MgCa(SiO_3)_2$) were used as starting powders. The amount and type of impurities in α-Al_2O_3 are shown in Table 1. Diopside is composed of SiO_2 (55 wt.%), CaO (24 wt.%) and MgO (18 wt.%). The compositions and mechanical properties

* Corresponding author. Tel.: +86 412 576 8099.
E-mail addresses: hester5371@gmail.com (C. Liu), jhzhang@sdu.edu.cn (J. Zhang).
[1] Tel.: +86 531 82266727.

0955-2219/$ – see front matter © 2007 Elsevier Ltd. All rights reserved.
doi:10.1016/j.jeurceramsoc.2007.05.023

Table 1
The amount and type of impurities in α-Al_2O_3

Raw materials	Impurities (mass fraction, ppm) ≤							
α-Al_2O_3	K	Na	Ca	Mg	Fe	Si	Ti	Cu
	10	9	4	2	5	10	4	3

of pressureless sintered alumina matrix ceramics are listed in Table 2 (The suffix in AD_0, AD_3, AD_6 and AD_{12} represents the volume content of diopside. For example, AD_0 means the volume content of diopside is zero).

The raw materials were blended together according to their proportions and ball milled for 60 h in an alcohol medium to obtain a homogeneous mixture. Then the slurry was dried in vacuum and screened. Green bodies (50 mm × 50 mm × 50 mm) were shaped using isostatic cold pressing technology in rubber molds. Lastly, the green bodies were sintered at 1520 °C (heating rate: 20 °C/min) for 140 min in N_2 atmosphere using pressureless sintering method.

2.2. Characterization

Test specimens with nominal dimensions of 3 mm × 4 mm × 36 mm were cut from the pressureless sintered bodies. Densities of the specimens were measured by Archimedes method. Vickers hardness was measured on polished surface with a load of 9.8 N for 5 s with a micro-hardness tester (produced by Shanghai Hengyi electronic testing instrument corporation). Fracture toughness measurement was performed using indentation method. The indentations on sample surfaces were generated in a hardness tester (produced by Shandong Yexian material tester corporation), and the formula proposed by Cook and Lawn[8] was used to calculate the final fracture toughness.

2.3. Friction and wear tests

Friction and wear tests were carried out in a block-on-ring abrasion apparatus (MRH-3). The contact schematic diagram for frictional couple is shown in Fig. 1. A plain carbon steel ring (HRC 38–45) with outer diameter of 50 mm, inner diameter of 35 mm and thickness of 10 mm, was used as the counterpart. The investigated ceramics were cut into specimens with dimensions of 5 mm × 8 mm × 16 mm. The specimens were ground and polished with diamond paste to an average surface roughness of 0.1 μm. Sliding was performed under ambient conditions of temperature and humidity over a period of 30 min. For all tests, rotation speeds of 40, 80, 120 and 160 rpm were applied. The

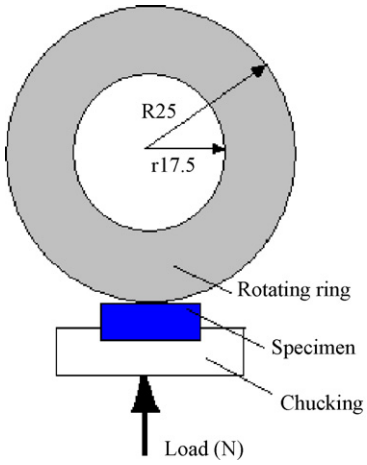

Fig. 1. Contact schematic diagram for the frictional couple.

normal load ranged from 50 to 200 N, corresponding to a contact pressure of about 5–15 MPa.

The friction coefficient is calculated according to the equation as follows

$$\mu = \frac{M}{P \times R} = \frac{F}{P} \tag{1}$$

where μ is friction coefficient, M is force moment of friction, R is the outer radius of carbon steel ring (25 mm), P refers to the normal load (N) and F to friction force (N). P and F can be directly attained from the digital display of the apparatus.

The wear rate is obtained by the following formula

$$\omega = \frac{V}{L \times P} \tag{2}$$

In this equation, ω is wear rate ($m^3\,N^{-1}\,m^{-1}$), V is volume loss of the test specimens (m^3) and L refers to the sliding distance (m).

The volume loss V of the block specimens in Eq. (2) is calculated and determined by the expression[9]

$$V = \frac{BR^2}{a-b}\left[a\sin^{-1}\frac{a}{2R} + \sqrt{4R^2-a^2} - b\sin^{-1}\frac{b}{2R} - \sqrt{4R^2-b^2}\right] + \frac{2B}{3(a-b)}\left[\left(R^2-\frac{b^2}{4}\right)^{3/2} - \left(R^2-\frac{a^2}{4}\right)^{3/2}\right] \tag{3}$$

where B is the width of the test specimens (m), a and b refers to the dimensions of the wear traces on the block specimens,

Table 2
Compositions and mechanical properties of pressureless sintered alumina matrix ceramics

Specimens	Compositions (vol.%)	Relative density(%)	Hardness (GPa)	Fracture toughness (MPa $m^{1/2}$)
AD_0	100% Al_2O_3	88.6	7.3	4.1
AD_3	97% Al_2O_3 + 3% diopside	97.2	15.6	5.2
AD_6	94% Al_2O_3 + 6% diopside	97.5	13.7	5.3
AD_{12}	88% Al_2O_3 + 12% diopside	97.9	13.5	5.0

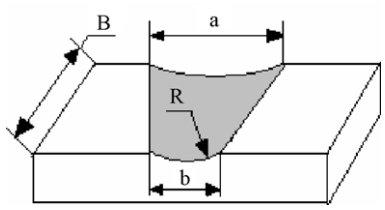

Fig. 2. Schematic diagram of wear traces on the block specimens.

Table 3
Friction coefficient of AD_0 specimen

Rotation speeds (rpm)	Normal load (N)			
	50	100	150	200
40	0.7619	0.7475	0.7065	0.6630
80	0.7485	0.7236	0.6382	0.6238
120	0.7172	0.6780	0.6550	0.6005
160	0.6972	0.6164	0.5820	0.5391

shown in Fig. 2 and measured with a digital-reading microscope (JC-10). The average of three replicate test results is adopted in order to minimize data scattering and decrease the relative error.

Finally, the surfaces of the worn specimens were examined by scanning electron microscopy (HITACHI S-570).

3. Results and discussion

3.1. Tribological behaviour: friction coefficient and wear rate of the experiments

The measured friction coefficients of AD_0, AD_3, AD_6 and AD_{12} at different normal loads and rotation speeds are shown in Tables 3–6, respectively. Each table shows the same trend: a general decrease in the coefficient of friction with increasing the normal load or rotation speed. During the friction and wear tests, the increasing of rotation speed or normal load conduces to improve the surface roughness of specimen and enlarge the contact area. The higher the rotation speed or normal load is, the larger the shearing stress in contact area will be, and as a result, the temperature of contact area may increase distinctly, making the plastic deformation in contact area more easier. Thus the friction coefficient decreases with increasing the rotation speed or normal load. Compare Table 3 with Tables 4–6, it can be seen that the friction coefficient of pure alumina is in the range of 0.53–0.76, and that of fine alumina matrix ceramic materials toughened by diopside is in the range of 0.44–0.69, smaller than that of pure alumina, indicating that introduction of diopside decreases the friction coefficient of pressureless sintered fine alumina matrix ceramic composites.

Table 4
Friction coefficient of AD_3 specimen

Rotation speeds (rpm)	Normal load (N)			
	50	100	150	200
40	0.6322	0.6009	0.6161	0.7018
80	0.6104	0.5924	0.5857	0.5699
120	0.5893	0.5859	0.5575	0.5417
160	0.5438	0.5361	0.5317	0.5106

Table 5
Friction coefficient of AD_6 specimen

Rotation speeds (rpm)	Normal load (N)			
	50	100	150	200
40	0.6912	0.6473	0.5484	0.5532
80	0.6757	0.6079	0.5165	0.5198
120	0.6500	0.5381	0.4930	0.4590
160	0.6068	0.5140	0.4728	0.4423

Table 6
Friction coefficient of AD_{12} specimen

Rotation speeds (rpm)	Normal load (N)			
	50	100	150	200
40	0.6490	0.6368	0.6262	0.6018
80	0.6318	0.6243	0.5800	0.5628
120	0.5833	0.5509	0.5113	0.5049
160	0.5600	0.4928	0.4900	0.4738

The measured wear rate of AD_0, AD_3, AD_6 and AD_{12} are plotted in Figs. 3–6 as a function of the normal load tested at different speeds under dry sliding. As can be seen from Figs. 3–6 that the wear rates for all test specimens increased with increas-

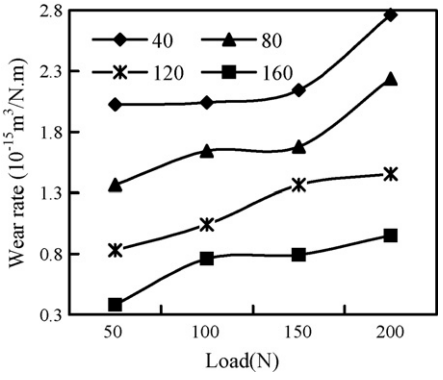

Fig. 3. Variation of wear rate for AD_0 specimen with normal load and rotation speed.

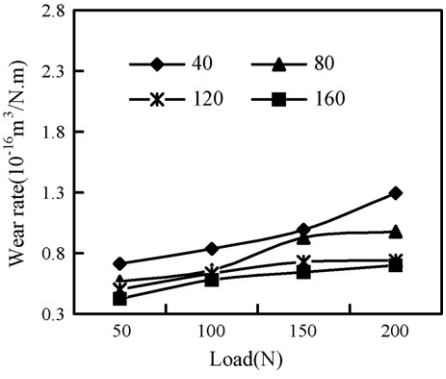

Fig. 4. Variation of wear rate for AD_3 specimen with normal load and rotation speed.

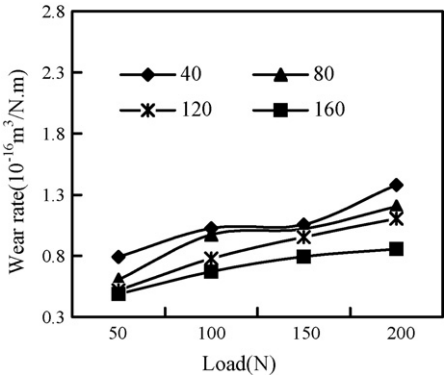

Fig. 5. Variation of wear rate for AD_6 specimen with normal load and rotation speed.

ing the normal load. While this trend of increase are not linear and are always accompanied with a jump of wear rate, induced by wear transition. As we all know that higher rotation speed lowers the wear transition load, the similar trends of higher speed causing higher wear and lower wear transition load were observed for pressureless sintered fine structural alumina matrix ceramic materials. Wear transition may be also in relevant to the variation of wear mechanism, generally changing form mild wear to severe wear. There are essential differences between effects of normal load and rotation speed on wear transition. When normal load increases, the stress in contact area, exceeding critical stress, leads to formation and propagation of crack on the surface of block specimen, fracture of severe wear may come into being. The influences of speed on wear and wear transition are more complicated and usually attributed to the effect of speed on the surface temperature. High surface temperature brought by high sliding speed and smart friction, which, in turn, may be the reason for wear rate reduction. It can be generally concluded that, the larger the normal load is applied, the earlier the wear transition occurs and the more severe the wear will be, and also, the higher the temperature, the lower the wear transition loads. This conclusion is similar with that drawn by Yushu Wang.[10]

Fine alumina matrix ceramic materials toughened by diopside show low wear rate of magnitude 10^{-16} m^3/N m, smaller than pure alumina (10^{-15} m^3/N m) abrasive wear. Obviously, introduction of diopside into alumina matrix results in signifi-

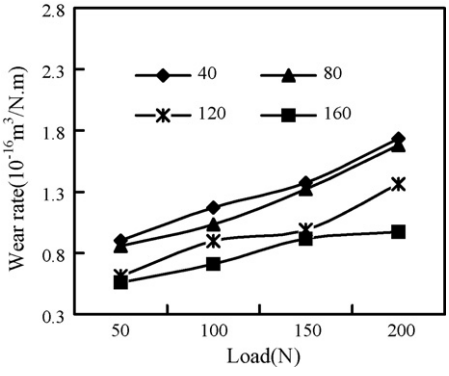

Fig. 6. Variation of wear rate for AD_{12} specimen with normal load and rotation speed.

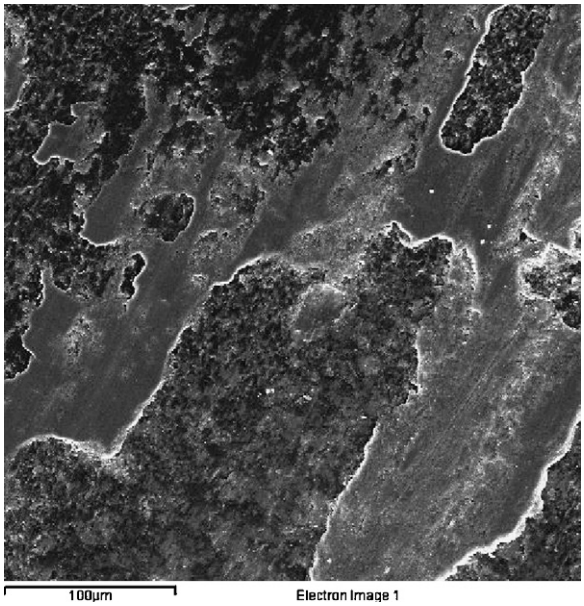

Fig. 7. SEM micrographs of wear track on AD_3 under dry sliding conditions (normal load: 50 N, rotation speed: 160 rpm).

cant improvement in tribological properties of the composites. The major reason may be that, addition of diopside obviously prompts the sintering of diopside-reinforced composites, the relative density of composites reaches ≈97.9% as the content of diopside is 12 vol.%. Based on this good densification rate, improved mechanical properties have been obtained. As a result, tribological properties of the diopside-reinforced composites are improved significantly.

3.2. Tribological behaviour: wear mechanisms

Figs. 7 and 8 show the SEM micrographs of worn surfaces of AD_3 specimen tested at normal loads of 50 and 200 N, respec-

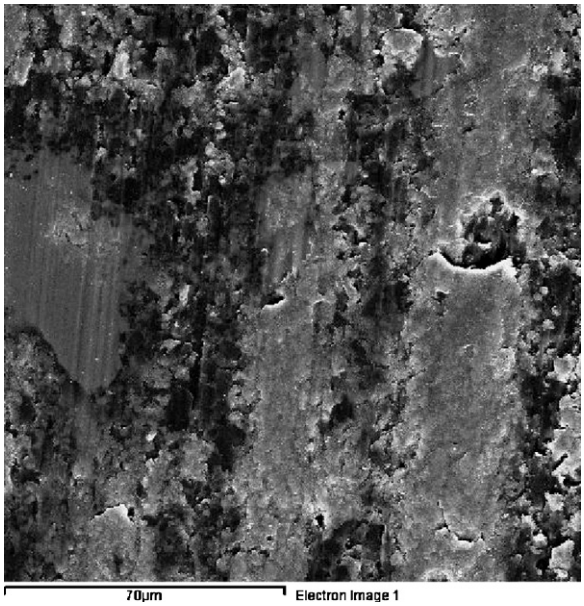

Fig. 8. SEM micrographs of wear track on AD_3 under dry sliding conditions (normal load: 200 N, rotation speed: 160 rpm).

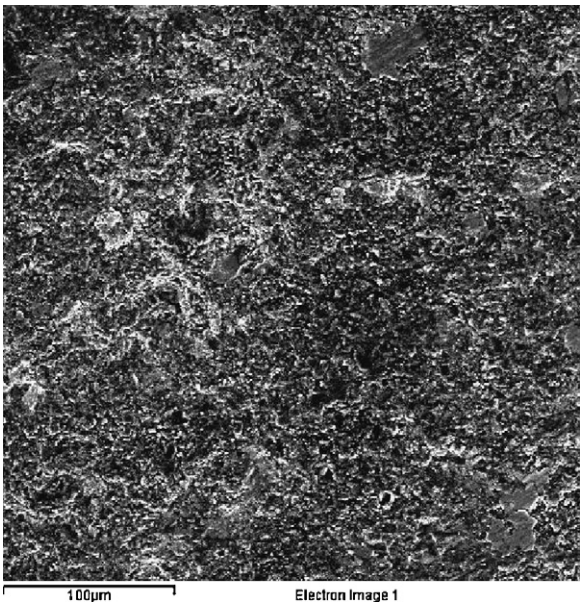

Fig. 9. SEM micrographs of wear track on AD_6 under dry sliding conditions (normal load: 50 N, rotation speed: 160 rpm).

tively. As can be seen from Fig. 7, the worn area of the AD_3 tested at lower load (50 N), was relatively smooth and covered with continuous transfer films, which may be transferred from the carbon steel ring. There is no distinct evidence of surface cracks in Fig. 7, which may be due to the fact that the wear is steady and the test specimen is in mild wear regime. After being tested at higher load (200 N), however, the worn area is covered by wear debris, and some isolated grain pull-out occurs in the worn surface (Fig. 8), indicating that a transition from mild to severe wear occurred as the normal load increased from 50 to 200 N. SEM micrographs of worn surfaces of AD_6 specimen tested at normal loads of 50 and 200 N are shown in Figs. 9 and 10, respectively. The worn surfaces of AD_6 specimen are also relatively smooth and few cracks can be detected. Clearly, such a phenomenon can be attributed directly to the fact that AD_6 specimen has a larger value of fracture toughness compared with AD_3 specimen (see Table 2). In our previous work, it was concluded that the wear mechanisms of pure alumina might be brittle fracture and grain pull-out.[2] It can be concluded from the above analysis that the dominant wear mechanism of the fabricated composites was mechanical interlocking combined with a little micro-fracture and grain pull-out.

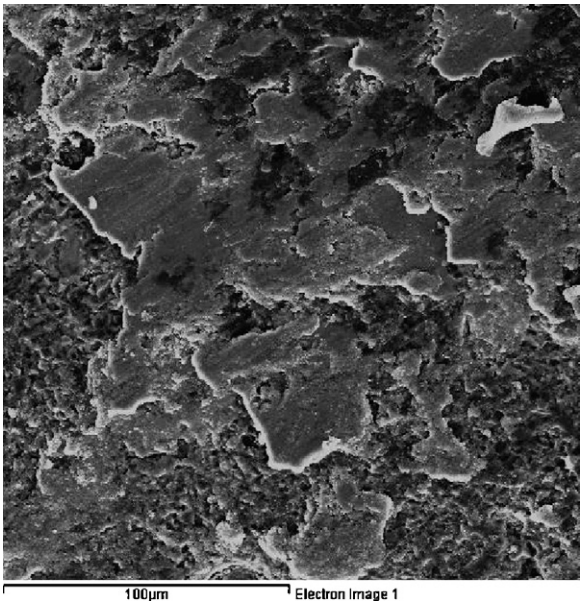

Fig. 10. SEM micrographs of wear track on AD_6 under dry sliding conditions (normal load: 200 N, rotation speed: 160 rpm).

4. Conclusion

Fine structural alumina matrix ceramic materials are fabricated by pressureless sintering technology. The friction and wear behaviour of fine structural alumina matrix ceramic composites, coupled with carbon steel ring, were investigated using a block-on-ring apparatus in unlubricated conditions, in air, at room temperature, at different sliding speed and load. The most useful result was found, where, the friction coefficient values and wear rate of alumina matrix ceramic composites toughened by diopside are lower than that of pure alumina. The wear rate of pure alumina was in the order of 10^{-15} $m^3/N\,m$ while that of alumina matrix ceramic composites toughened by diopside was 10^{-16} $m^3/N\,m$. In conclusion, introduction of diopside into alumina decreases its wear rate and coefficient of friction, and the wear rate increases with the increase in load value. The dominant wear mechanism of the fabricated composites was mechanical interlocking combined with a little micro-fracture and grain pullout.

Acknowledgements

The work described in this paper is supported by the Ministry of Education, PR China (No. 103101), the Outstanding Young Scientist Rewards of Shandong Province (No. 03BS103) and (No. 2005BS04008).

References

1. Liu, Changxia, Zhang, Jianhua, Sun, Junlong *et al.*, Pressureless sintering of large-scale fine structural alumina matrix ceramic guideway materials. *Mater. Sci. Eng.*, 2007, **A444**, 58–63.
2. Zhang, Xihua, Liu, Changxia and Zhang, Jianhua, Study on the friction and wear performance of alumina matrix ceramic materials reinforced by AlTiC. *J. Shandong Univ. (Eng. Sci.)*, 2005, **35**(4), 5–8 (in Chinese).
3. Kerkwijk, Bas, Garcĭýa, Monserrat, van Zyl, Werner E. *et al.*, Friction behaviour of solid oxide lubricants as second phase inα-Al_2O_3 and stabilised ZrO_2 composites. *Wear*, 2004, **256**, 182–189.
4. Ucar, V., Ozel, A., Mimaroglu, A. *et al.*, Influence of SiO_2 and MnO_2 additives on the dry friction and wear performance of Al_2O_3 ceramic. *Mater. Des.*, 2001, **22**, 171–175.
5. Esposito, L. and Tucci, A., Microstructure dependence of friction and wear behaviours in low purity alumina ceramics. *Wear*, 1997, **205**, 88–96.
6. Taktak, S. and Baspinar, M. S., Wear and friction behaviour of alumina/mullite composite by sol–gel infiltration technique. *Mater. Des.*, 2005, **26**, 459–464.

7. Gong, Jianghong, Miao, Hezhuo and Zhao, Zhe, Effect of TiC-particle size on sliding wear of TiC particulate reinforced alumina composites. *Mater. Lett.*, 2002, **53**, 258–261.
8. Cook, R. F. and Lawn, B. R., A modified indentation toughness technique. *J. Am. Ceram. Soc.*, 1983, **66**(11), 200–201.
9. Gao, Caiqiao and Liu, Jiajun, *Adhesive Abrasion and Fatigue Wear of Material*. Mechanical Industry Press, Peking, China, 1989, pp. 80–243.
10. Wang, Yushu and Hsu, Stephen M., The effects of operating parameters and environment on the wear and wear transition of alumia. *Wear*, 1996, **195**, 90–99.